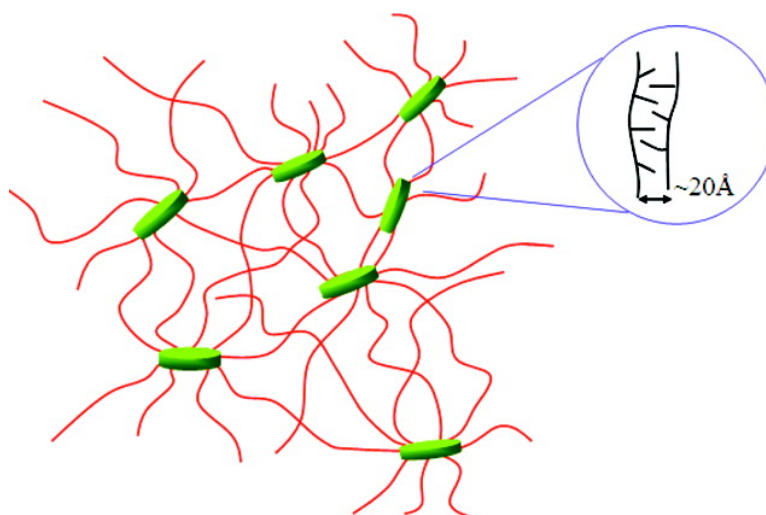Article

Scattering Study of the Conformational Structure and Aggregation Behavior of a Conjugated Polymer Solution

Yen-Cheng Li, Chun-Yu Chen, Ying-Xun Chang, Pei-Ying Chuang, Jean-Hong Chen,
Hsin-Lung Chen, Chain-Shu Hsu, Viktor A. Ivanov, Pavel G. Khalatur, and Show-An Chen

More About This Article

Additional resources and features associated with this article are available within the HTML version:

- Supporting Information
- Access to high resolution figures
- Links to articles and content related to this article
- Copyright permission to reproduce figures and/or text from this article

View the Full Text HTML

Scattering Study of the Conformational Structure and Aggregation Behavior of a Conjugated Polymer Solution

Yen-Cheng Li,[†] Chun-Yu Chen,[‡] Ying-Xun Chang,[§] Pei-Ying Chuang,[§] Jean-Hong Chen,*[,§] Hsin-Lung Chen,*[,‡] Chain-Shu Hsu,[†] Viktor A. Ivanov,[‖] Pavel G. Khalatur,[⊥] and Show-An Chen[‡]

[†]*Department of Applied Chemistry, National Chiao Tung University, Hsin-Chu 30050, Taiwan,* [‡]*Department of Chemical Engineering, National Tsing Hua University, Hsin-Chu 30013, Taiwan,* [§]*Department of Polymer Materials, Kun Shan University, Yung-Kang City, Tainan Hsien 71003, Taiwan,* [‖]*Physics Department, Moscow State University, Moscow 119991, Russia and* [⊥]*Institute of Organoelement Compounds, RAS, Moscow 119991, Russia*

Received October 13, 2008. Revised Manuscript Received December 26, 2008

The conformational structure and the interchain aggregation behavior of a semirigid conjugated polymer bearing a decyl side chain, poly(2,3-diphenyl-5-decyl-1,4-phenylenevinylene) (DP10-PPV), in solutions with chloroform and toluene have been investigated by means of small-angle neutron scattering (SANS), static light scattering (SLS) and dynamic light scattering (DLS). The radius of gyration, persistence length, and the second virial coefficient of the polymer in dilute solution as determined by SLS were higher in chloroform than in toluene; consequently, the polymer assumed a more extended wormlike chain conformation in the former. The difference in the strength of interaction in the two solvents gave rise to contrasting aggregation behavior of the polymer in the semidilute regime. While only a minor fraction of the polymer underwent segmental association in chloroform, a considerable fraction of it formed clusters (microgels) with several micrometers in size in toluene. These clusters were further found to consist of sheetlike nanodomains. Compared with the DP-PPV bearing a shorter hexyl side chain, DP6-PPV, the aggregates of DP10-PPV in toluene were weaker as they could be easily disrupted by moderate heating. This was attributed to a lack of strong $\pi-\pi$ interaction between the DP10-PPV segments due to the greater steric hindrance imposed by the longer decyl side chains.

Introduction

Conjugated polymers have gained much interest because of their unique photophysical and semiconducting electrical properties leading to various opto-electronic applications, such as light-emitting diodes (LEDs) and photovoltaics.[1−3] This class of polymers possesses a semirigid or rigid backbone, and, without proper chemical modification, they are often infusible and insoluble in common organic solvents. This intractable nature can be circumvented by attaching flexible short side chains to the polymer backbone. Such a structural modification allows the polymers to be nominally soluble in common organic solvents such as chloroform and toluene, thus facilitating the device fabrication using spin or drop casting techniques.

The photophysical properties of conjugated polymers are strongly influenced by their chain conformation and the structure of the assembly of the polymer chains. The interchain assembly not only occurs in the bulk state but also in the solution. Previous spectroscopic and scattering studies have indicated that conjugated polymers undergo interchain aggregation easily in the solution state, even under large dilution (e.g., several weight percents).[4−7] However, the origin of this event and the structure of the resultant aggregates still remain the crucial issues to be resolved, as these aggregates affect the photophysics of these materials profoundly.[4,8−11]

Several studies have addressed the factors that control the conformational structure of conjugated polymers in solution. The delocalization of the conduction electrons in conjugated polymer systems and steric effects of the side chains serve to extend the polymer chain in solution. Aime et al. have found that the steric effect of the side chains induced significant expansion of the polymer chains.[12] The fact that such a steric effect played a strong role on the conformation of conjugated polymers has also been confirmed experimentally

*To whom correspondence should be addressed. E-mail: hslchen@mx.nthu.edu.tw (H.-L.C.); kelvench@mail.ksu.edu.tw (J.-H.C.).

(1) Burroughes, J. H.; Bradly, D. D. C.; Brown, A. R.; Marks, R. N.; Mackay, K.; Friend, R. H.; Burns, P. L.; Holmes, A. B. *Nature* **1990**, *347*, 539.

(2) Friend, R. H.; Gymer, R. W.; Holmes, A. B.; Burroughes, J. H.; Marks, R. N.; Taliani, C.; Bradley, D. D. C.; dos Santos, D. A.; Brédas, J. L.; Löglund, M.; Salaneck, W. R. *Nature* **1999**, *397*, 121.

(3) Spreitzer, H.; Becker, H.; Kluge, E.; Kreuder, W.; Schenk, H.; Demandt, R.; Schoo, H. *Adv. Mater.* **1998**, *10*, 1340.

(4) Nguyen, T. Q.; Doan, V.; Schwartz, B. J. *J. Chem. Phys.* **1999**, *110*, 4068.

(5) Grell, M; Bradley, D. D. C.; Ungar, G..; Hill, J.; Whitehead, K. S. *Macromolecules* **1999**, *32*, 5810.

(6) Collison, C. J.; Rotherberg, L. J.; Treemaneekarn, V.; Li, Y. *Macromolecules* **2001**, *34*, 2346.

(7) Hsu, J. H.; Fann, W. S.; Tsao, P. H.; Chuang, K. R.; Chen, S. A. *J. Phys. Chem. A* **1999**, *103*, 2375.

(8) Blatchford, J. W.; Jessen, S. W.; Lin, L. B.; Gustafson, T. L.; Fu, D. K.; Wang, H. L.; Swager, T. M.; MacDiarmid, A. G.; Epstein, A. J. *Phys. Rev. B* **1996**, *54*, 9180.

(9) Shi, Y.; Liu, J.; Yang, Y. *J. Appl. Phys.* **2000**, *87*, 4254.

(10) Peng, K. Y.; Chen, S. A.; Fann, W. S. *J. Am. Chem. Soc.* **2001**, *123*, 11388.

(11) Chen, S. H.; Su, A. C.; Huang, Y. F.; Su, C. H.; Peng, G. Y.; Chen, S. A. *Macromolecules* **2002**, *35*, 4229.
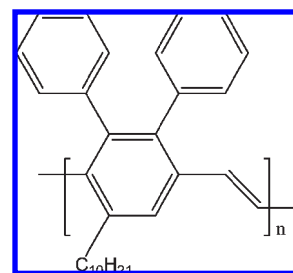
(12) Aime, J.P.; Ramakrishnan, S.; Chance, R.R.; Kim, M.W. *J. Phys. (Paris)* **1990**, *51*, 963.

from the solution properties of poly(alkythiophenes).[13−15] Gettinger et al. have reported that increasing the size of the solubilizing side chains increased the intrinsic persistence length of poly(phenylenevinylene) (PPV) backbone, and the resulting change in chain stiffness exerted a strong effect on the photoluminescence of the polymer.[16]

The aggregation behavior of a variety of conjugated polymers has also been investigated by small-angle neutron scattering (SANS). Perahia et al. utilized SANS to probe the aggregate structure of a conjugated polymer, poly(2,5-dinonylparaphenylene ethynylene) (PPE), in toluene solutions.[17,18] The triple bonds along the backbone imparted conformational rigidity to the molecule, making the PPE chains assume rodlike conformation. These rodlike molecules aggregated into large flat clusters driven by $\pi-\pi$ interaction below ca. 40 °C. When the aggregates were too large to move freely in the solution, a transition into a constrained or jammed phase took place, transforming the viscous solution into a gel. Poly(9,9-dioctylfluorene-2,7-diyl) (PF8) is another polymer whose aggregation behavior in solution state has been probed by SANS. It has been revealed that PF8 could be dissolved down to the molecular level in dilute (0.5−1.0 wt %) toluene solutions where they remained as stiff rods.[19] The polymer chains aggregated to form a network structure containing domains of aggregates of aligned segments in the semidilute toluene solution.[20] By contrast, the dissolution of PF8 only reached the colloidal level, giving rise to sheetlike aggregates in a poor solvent, methylcyclohexane (MCH).[19] A recent systematic study by Knaapila et al. on the effect of side chain length on the aggregation of polyfluorenes has revealed that the formation of sheetlike aggregates in MCH was rather universal, and the larger length scale structures of these sheets showed an odd−even dependence on the side length.[21]

Recently, we reported the interchain aggregation behavior of poly(2,3-diphenyl-5-hexyl-1,4-phenylenevinylene) (DP6-PPV) bearing hexyl side chains in the solutions with chloroform and toluene.[22] DP-PPVs have been considered as a family of green-emitting material for LED application due to their high glass transition temperature, high fluorescence efficiency and ease of monomer and polymer syntheses.[23−26] Using SANS, we have revealed that the aggregation of

(13) Heffner, G. W.; Pearson, D. S. *Macromolecules* **1991**, *24*, 6295.
(14) Spiegel, D. R. *Macromolecules* **1990**, *23*, 3568.
(15) Aime, J. P.; Bargain, F.; Schott, M.; Eckhardt, H.; Miller, G. G.; Elsenbaumer, R. L. *Phys. Rev. Lett.* **1989**, *62*, 55.
(16) Gettinger, C. L.; Heeger, A. J.; Drake, J. M.; Pine, D. J. *J. Chem. Phys.* **1994**, *101*, 1673.
(17) Perahia, D.; Traiphol, R.; Bunz, U. H. F. *J. Chem. Phys.* **2002**, *117*, 1827.
(18) Perahia, D.; Jiao, X.S.; Traiphol, R. *J. Polym. Sci., Part B* **2004**, *42*, 3165.
(19) Knaapila, M.; Garamus, V. M.; Dias, F. B.; Almásy, L.; Galbrecht, F.; Charas, A.; Morgado, J.; Burrows, H. D.; Scherf, U.; Monkman, A. P. *Macromolecules* **2006**, *39*, 6505.
(20) Rahman, M. H.; Chen, C. Y.; Liao, S. C.; Chen, H. L.; Tsao, C. S.; Chen, J. H.; Liao, J. L.; Ivanov, V. A.; Chen, S. A. *Macromolecules* **2007**, *40*, 6572.
(21) Knaapila, M.; Almásy, L.; Garamus, V. M.; Ramos, M. L.; Justino, L. L. G.; Galbrecht, F.; Preis, E.; Scherf, U.; Burrows, H. D.; Monkman, A. P. *Polymer* **2008**, *49*, 2033.
(22) Li, Y. C.; Chen, K. B.; Chen, H. L.; Hsu, C. S.; Tsao, C. S.; Chen, J. H.; Chen, S. A. *Langmuir* **2006**, *22*, 11009.
(23) Hsieh, B. R.; Antoniadis, H.; Bland, D.C.; Feld, W.A. *Adv. Mater.* **1995**, *7*, 36.
(24) Hsieh, B. R.; Yu, Y.; Forsythe, E. W.; Schaaf, G. M.; Feld, W. A. *J. Am. Chem. Soc.* **1998**, *120*, 231.
(25) Wan, W. C.; Antoniadis, H.; Choong, V. E.; Razafitrimo, H.; Gao, Y.; Feld, W. A.; Hsieh, B. R. *Macromolecules* **1997**, *30*, 6567.
(26) Hsieh, B. R.; Yu, Y.U.S. Patent 5,945,502, **1999**.

Scheme 1. Poly(2,3-diphenyl-5-decyl-1,4-phenylenevinylene) (DP10-PPV)

DP6-PPV in chloroform and toluene yielded network aggregates whose internal structure could be characterized by certain fractal dimensions. Two types of segmental association with distinct stability were identified for the toluene solution. The highly stable segmental association was attributed to the $\pi-\pi$ complex already present in the DP6-PPV powder, while the other type of labile segmental association was ascribed to the poor affinity of the aliphatic side chains of DP6-PPV to toluene.

Herein we report a comparative study of the conformational structure and aggregation behavior of a DP-PPV bearing a longer decyl side chain, i.e., poly(2,3-diphenyl-5-decyl-1,4-phenylenevinylene) (DP10-PPV). In conjunction with the previous results of DP6-PPV, we attempt to reveal the role of the side-chain length in the interchain assembly of DP-PPVs in the solution state. The chemical structure of DP10-PPV is shown in Scheme 1.

Intuitively, the incorporation of the longer decyl side chains in DP10-PPV should impose a stronger steric hindrance (relative to that of DP6-PPV) against the interchain aggregation of the polymer; therefore, the aggregate structure of DP10-PPV may be different from that of DP6-PPV. In addition to the aggregation behavior in the semidilute solution, the conformational structure of DP10-PPV in the dilute regime, where the interchain aggregation was not significant, has also been investigated by means of static light scattering (SLS) here. It will be shown that, although DP10-PPV displays a weaker tendency toward aggregation than DP6-PPV, this polymer is still able to aggregate in semidilute solutions, generating aggregates with hydrodynamic radii of submicrometer to 10 μm in size depending on the concentration. These aggregates are however loosely bound by the micelle-like association of segments that can be easily disrupted by moderate heating.

Experimental Section

Materials and Solution Preparation. DP10-PPV was synthesized according to the procedure described elsewhere.[23−26] The weight-average molecular weight (M_w) of the polymer was 463 000 g/mol as measured by SLS using chloroform solvent. The polymer solutions with the concentrations ranging from 0.001 to 1.0 wt % were prepared by dissolving an appropriate amount of the polymer in chloroform and toluene. The mixtures of the polymer and the solvent were stirred at ca. 40 °C for 12 h, where macroscopically homogeneous solutions were observed by the naked eye after the stirring. d-Solvents were used for preparing the solutions for SANS study to enhance the contrast in neutron scattering length densities (SLDs).

SANS Measurements. The SANS measurements were performed on the 8 m SANS instrument (NG1) at the National

Institute of Standard and Technology (NIST).[27] The incident neutron wavelength was $\lambda = 8$ Å with a wavelength dispersion of $\Delta\lambda/\lambda = 0.14$. The configuration of the SANS instrument, including the collimated pinhole size and the sample-to-detector distance, was optimized to give an effectively measured q-range of 0.008 Å^{-1} to 0.12 Å^{-1}. The scattering intensity $I(q)$ was corrected for transmission, background, and parasitic scattering and normalized to an absolute intensity (scattering cross section per unit sample volume) as a function of the scattering vector q where q = $(4\pi/\lambda) \sin(\theta/2)$ (θ is the scattering angle).[28] The incoherent backgrounds from the pure solvents were also measured, corrected by the volume fraction displaced by the dissolved DP10-PPV, and subtracted from the reduced SANS data. The temperature (calibrated and controlled within ± 0.1 °C) of the solution during SANS measurement was achieved by use of a 10-piston heating/cooling block connected to a circulating bath (50/50 mixture of water and ethylene glycol). For the measurement at each temperature, the sample was first held at the prescribed temperature for 30 min followed by data acquisition for another 30 min. This acquisition time was sufficient to give reasonable counting statistics of the scattered intensity ($\sim 10^6$ counts).

SLS Measurements. The SLS measurements were carried out using an ALV/CGS-3 light scattering spectrometer equipped with an ALV/LSE-5003 multiple-τ digital correlator. A JDS-Uniphase solid-state He−Ne laser having the output power of ca. 22 mW at the operating wavelength of 632.8 nm was used as the light source. The reciprocal reduced scattering intensity, Kc/R_θ was obtained, where c is the concentration of polymer and R_θ is the reduced intensity. The optical constant K for vertically polarized light was calculated according to K = $4\pi^2 n_0^2 (dn/dc)^2/N_A\lambda^4$, where n_o is the refractive index of the solvent, dn/dc is the refractive index increment with respect to concentration, λ is the wavelength of light in vacuum, N_A is Avogadro's constant, and θ is the scattering angle. The second virial coefficient, A_2, the z-average radius of gyration, R_g, and the weight-average molecular weight, M_w, are related to Kc/R_θ via the well-known Zimm equation.[29,30]

$$\frac{Kc}{R_\theta} = \frac{1}{M_w}\left[1 + \frac{16}{3}\pi^2 n_0^2 \frac{R_g^2}{\lambda^2} \sin^2(\theta/2) + ...\right] + $$
$$2A_2 c + ... \quad (1)$$

The values of the refractive index increment, dn/dc, for DP10-PPV in chloroform and toluene solutions at 25 °C were 0.262 and 0.314 mL/g, respectively, as measured by an Optilab DSP differential refractometer (Wyatt Tech. Co.) with a laser wavelength of 632.8 nm.

Dynamic Light Scattering (DLS) Measurements. DLS experiments were also performed using the ALV/CGS-3 light scattering spectrometer equipped with an ALV/LSE-5003 multiple-τ digital correlator. The laser beam was passed through a quartz cell holding the solutions, and the scattering intensity was detected at various angles with respect to the incident beam. The autocorrelation function of the light scattering intensity, $G(q,t) = \langle I(q,t)I(q,0)\rangle/\langle I(q,0)^2\rangle$, with $I(q,0)$ being the mean intensity at a scattering vector q, was measured using an automated ALV goniometer with an ALV/LSE-5003 multiple-τ digital correlator over the time range of 10^{-8}–10^3 s. For an ergodic (fluid-like) system, the

normalized intensity autocorrelation function $g^2(t)$ can be directly related to the normalized electric autocorrelation function $g^{(1)}(t)$ via the Sigeret relation as shown in eq 2.[31,32]

$$g^{(2)}(t) = 1 + \beta|g^{(1)}(t)|^2 \quad (2)$$

where the parameter β denotes the zero lag-time limit of the normalized correlation and is hence known as the intensity intercept. The values of β are 0.5−0.9 for typical DLS experiments. For a system exhibiting a distribution of collective motions, $g^{(1)}(t)$ can be represented by the superposition of exponential decay functions. The Laplace inversion routine of $g^{(1)}(t)$ was performed to yield the distribution of relaxation times $A(\tau)$, viz.,

$$g^{(1)}(t) = \int_0^\infty A(\tau) \exp(-t/\tau)d\tau \quad (3)$$

The translational diffusion coefficient distribution was obtained from $A(\tau)$, and the hydrodynamic radius distribution was eventually obtained using the Stokes−Einstein equation, $R_h = k_B T/(6\pi\eta D)$, where k_B is the Boltzman constant, T is the absolute temperature, D is the diffusion coefficient, and η is the solvent viscosity.

Results and Discussion

1. Conformational Structure of DP10-PPV in Dilute Solutions Studied by SLS. The solvent quality mentioned in most studies of conjugated polymer solutions is only phenomenological, lacking an actual estimate of the quality. The value of the second virial coefficient, A_2, obtained from the Zimm plot of SLS data can be regarded as a measure for the strength of polymer−solvent interaction in dilute solutions. Here we have measured the A_2 and the radius of gyration, R_g, of DP10-PPV in solutions with chloroform and toluene. Figure 1 shows the Zimm plots of DP10-PPV in dilute solutions with chloroform and toluene at 25 °C. The concentrations studied range between 0.001 and 0.1 wt %, which falls below the overlap concentration ($c^* =$ ca. 0.33 and 0.43 wt % for chloroform and toluene solutions, respectively, as estimated via $c^* \sim 3M/4\pi N_A(R_g)^3$, with M being the molecular weight of the polymer). The Zimm plots of both types of solutions display good linearity, indicating that the individual DP10-PPV chains in both dilute solutions are well dispersed. The values of A_2 and R_g obtained through the extrapolation to zero concentration and zero angle, respectively, are listed in Table 1. It can be seen that the value of A_2 obtained for chloroform solution, ca. 6.7×10^{-6} mol dm^3 g^{-2}, is larger than that (ca. 3.7×10^{-6} mol dm^3 g^{-2}) for toluene solution, indicating that the attractive force between DP10-PPV and chloroform is stronger than that between DP10-PPV and toluene. This finding is consistent with our theoretical calculations of the thermodynamic phase diagram of DP6-PPV (another DP-PPV bearing a hexyl side chain) solutions with chloroform and toluene (see Supporting Information). The difference in the polymer−solvent interaction of DP10-PPV in the two solvents is expected to affect the conformational structure and the aggregation behavior of DP10-PPV in the solutions.

(27) Glinka, C. J.; Barker, J. G.; Hammouda, B.; Krueger, S.; Moyer, J. J.; Orts, W. J. *J. Appl. Crystallogr.* **1998**, *31*, 430.

(28) Cold Neutron Research Facility at the National Institute of Standard and Technology, *NG3 and NG7 30-Meter SANS Instruments Date Acquisition Manual*; NIST: Gathersburg, MD, **1999**.

(29) Zimm, B. H. *J. Chem. Phys.* **1948**, *16*, 1093.

(30) Zimm, B. H. *J. Chem. Phys.* **1948**, *16*, 1099.

(31) Schmitz, K. S. *An Introduction to Dynamic Light Scattering by Macromolecules*; Academic Press: Boston/San Diego/New York, **1990**.

(32) Brown. W. *Dynamic Light Scattering*; Clarendon Press: Oxford, **1993**.
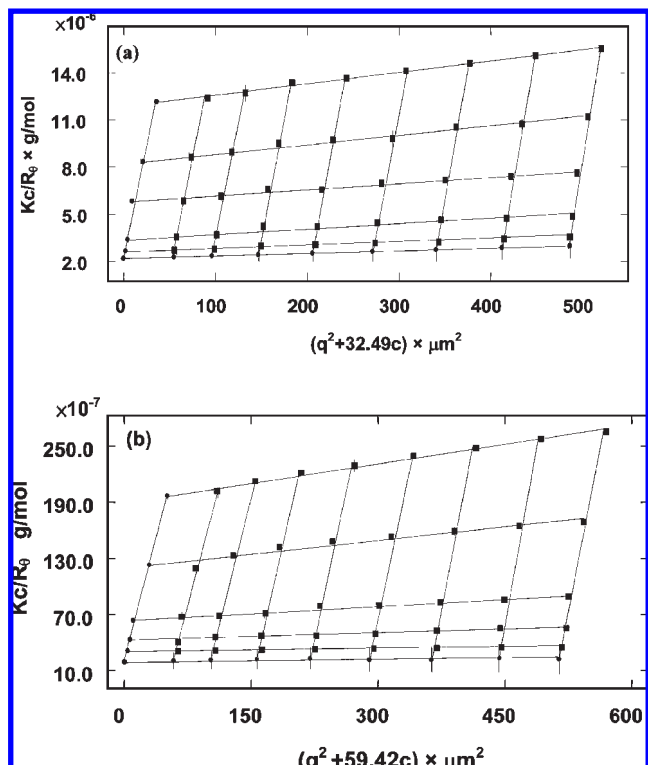
Figure 1. Zimm plots of DP10-PPV in dilute solutions at (25 ± 0.1) °C: (a) DP10-PPV/chloroform dilute solutions and (b) DP10-PPV/toluene dilute solutions.

Table 1. The Conformational Parameters of DP10-PPV in Dilute Solutions Obtained from Eqs 4 Using SLS Data at 25 °C[a]

	A_2 (mol dm^3 g^{-2})	R_g (nm)	l_p (nm)
DP10-PPV/chloroform	6.7×10^{-6}	38	6.5
DP10-PPV/toluene	3.7×10^{-6}	35	5.5

[a] [M_w = 463 kg/mol; M_0 = 394 g/mol; l_0 = 5.7 Å].

The former effect is evidenced by the slightly larger R_g in chloroform solution than that in toluene.

Knowing the value of R_g, the persistence length, l_p, of DP10-PPV can be calculated using the Kratky−Porod wormlike chain model,[16,33] which prescribes the R_g as

$$R_g{}^2 = \frac{l_p L}{3} = \frac{l_p l_o M}{3 M_o} \qquad (4)$$

where L is the contour length of the polymer, M_o is the monomer molecular weight, and l_o is the monomer length. The molecular weight of DP10-PPV used in this study is 463 000 g/mol, and the monomer molecular weight and length are 394 g/mol and 5.7 Å, respectively. The contour length of the DP10-PPV chain calculated from its molecular weight and monomer length is hence ca. 670.5 nm. The values of l_p calculated from eq 4 for DP10-PPV in chloroform and toluene dilute solutions are tabulated in Table 1. Here we should note that eq 4 is valid for an ideal chain or for a chain with excluded volume but under θ conditions, and therefore the data for the persistence length in Table 1 should be considered as a rough estimation to demonstrate the trend, namely, the values only represent the apparent

persistence length. This persistence length is found to be larger for the polymer in chloroform, showing that the polymer chains are stiffer or more expanded in this better-quality solvent. Our theoretical calculations based on the microscopic atomistic model for calculation of interaction potential between effective monomer units, which is then combined with the Flory−Huggins model (see the Supporting Information), also support our statement that the apparent persistence lengths in both solvents are indeed attributable to the difference in thermodynamic solvent quality.

2. Conformational Structure and Aggregation Behavior of DP10-PPV in Semidilute Solutions Studied by SANS. We found that the solutions with concentrations lying above 0.1 wt % are able to give rise to neutron scattering intensities with reasonably good signal-to-noise ratio. In this case, the conformational and aggregate structure of the polymer chains may be elucidated directly from the SANS intensity profiles.

Figure 2 shows the room-temperature SANS profiles of DP10-PPV in chloroform solutions at three different concentrations. The SANS intensities follow $I(q) \sim q^{-1}$ dependence in the high-q region ($q > \sim 0.03$ Å^{-1}), irrespective of the polymer concentration due to the rodlike nature of the segments constituting the DP10-PPV chains.[22,34] In the low-q region ($q < 0.03$ Å^{-1}), the scattering intensities are found to exhibit upturns. Such an upturn may be due to the aggregation of the chain segments or associated with the crossover of the wormlike conformation of the well-dispersed polymer chains from the rodlike character under larger spatial resolution to the flexible regime under smaller spatial resolution.[35] The contribution of interchain aggregation to the intensity upturn is indeed unlikely considering that the intensities are quite weak (with the order of magnitude of 10^{-2} cm^{-1} comparing to 10^{-1} cm^{-1} for 0.1 wt % DP6-PPV/chloroform solution showing obvious interchain aggregation). Moreover, when the intensities are normalized by the overall polymer concentration (see Supporting Information), the normalized intensities of 0.5 and 1.0 wt % solutions are indeed lower than that of 0.1 wt % solution in the low-q region (i.e., the increase in the scattering intensity is less than that prescribed by the concentration increase). If the interchain aggregation dominated the low-q intensity upturn, the opposite trend should have been observed as a result of stronger aggregation power at higher polymer concentrations. Therefore, we consider the whole scattering curves in Figure 2 to be dominated by the form factor of the DP10-PPV wormlike chains. In other words, most DP10-PPV chains are well dispersed in chloroform.

The SANS profiles in Figure 2 are fitted by the wormlike chain model with excluded volume interaction. In this model, the polymer chain is treated as a flexible cylinder with a circular cross section and a uniform SLD. The non-negligible diameter of the cylinder is included by accounting for the excluded volume interaction[36,37] (the expression of the scattering intensity of this model can be found in the Supporting Information). The fitting results are displayed by the solid curves superposing on the experimental scattering profiles,

(33) Kratky, O.; Porod, G. *Recl. Trav. Chim. Pays−Bas* **1949**, *68*, 1106.

(34) Ou-Yang, W. C.; Chang, C. S.; Chen, H. L.; Tsao, C. S.; Peng, K. Y.; Chen, S. A.; Han, C. C. *Phys. Rev. E* **2005**, *72*, 031802.
(35) Higgins, J. S.; Benoit, H. C. *Polymers and Neutron Scattering*; Clarendon Press: Oxford, **1994**.
(36) Pedersen, J. S.; Schurtenberger, P. *Macromolecules* **1996**, *29*, 7602.
(37) Chen, W. R.; Butler, P. D.; Magid, L. J. *Langmuir* **2006**, *22*, 6539.
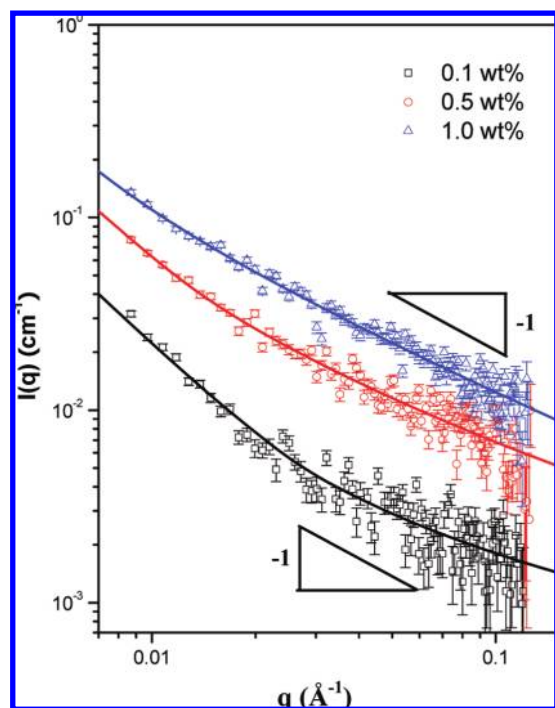
Figure 2. Room-temperature SANS profiles of DP10-PPV in chloroform solutions at different concentrations. The intensity exhibits a power law of $I(q) \sim q^{-1}$ in the high-q region corresponding to the form factor of the rodlike segments in the chains. The solid curves represent the fits using the wormlike chain model with excluded volume interaction. The fitting parameters are tabulated in Table 2.

Table 2. The Conformational Parameters of DP10-PPV in Semidilute Solutions with Chloroform Obtained from Fitting the SANS Profiles Using the Wormlike Chain Model with Excluded Volume Interaction[a]

polymer concentration (wt %)	l_p (nm)	R (nm)[b]
0.1	6.4	0.41
0.5	13.3	0.46
1.0	23.0	0.52

[a] The contour length was fixed at 670.5 nm for the fittings. [b] Radius of the polymer chain segments assuming circular cross section.

SPA-300HV atomic force microscope operated under the tapping mode. Figure 3 displays the corresponding topographic AFM image. The dispersed wormlike coil structure several micrometers in size is observed over a large area. However, some segmental associates formed by the interpenetration of numerous threads, presumably of the DP10-PPV chains, are also observed. The average height of the segmental associates is ca. 2.0 nm. In a work on the visualization of the single chain of a monodendron-jacketed polymer, Sheiko et al. have found that the height of a monolayer of the polymer was about (1.2 ± 0.2) nm.[38] Because each repeat unit of the polymer carries a bulky side group attached with three tetradecyl chains, which are longer than the decyl side chains of DP10-PPV, the height of a monolayer of DP10-PPV chains is expected to be lower than 1.2 nm. So the height of 2.0 nm indicates that the segmental associates observed in Figure 3 are formed by the interpenetration of more than one layers of DP10-PPV chains, and the solution concentration used for the casting is probably still quite high.

We now turn to the structure of DP10-PPV in the poorer solvent, toluene. Figure 4 shows the SANS profiles of DP10-PPV/toluene solutions at three concentrations. In contrast to the chloroform solutions, here the q-dependence of the intensity is found to transform to the power law of q^{-2} at the higher concentrations of 0.5 and 1.0 wt % over nearly the entire q range studied. The DLS study, to be discussed in the next section, shows the clear presence of a slow relaxation mode of the polymer at these two concentrations, which signals the aggregation of a significant fraction of the polymer chains to form clusters. Therefore, the SANS intensities at 0.5 and 1.0 wt % are considered to be dominated by the aggregates formed in toluene. This postulate is corroborated by comparing the intensity profiles normalized by the SLD contrast of the toluene solutions with those of the chloroform solutions, as shown in Figure 5. It can be seen that the 0.5 and 1.0 wt % toluene solutions consistently exhibit a stronger contrast-normalized intensity in the low-q region, which signals that DP10-PPV chains undergo aggregation to a significant extent in toluene. In this case, the observed q^{-2} dependence of the intensity is not associated with the wormlike chain conformation under θ condition, in that the contrast-normalized intensity of toluene solution in the low-q region (e.g., 0.01 Å^{-1}) is about 6 times that of the chloroform solution in which the individual wormlike chains are well dispersed. It is further noted that the hydrodynamic radius associated with the aggregate relaxation measured by DLS is of micrometer scale; consequently, the SANS intensities recorded in the present q range are mainly contributed by the internal structure of the micrometer-sized aggregates.

and the numerical values of the fitting parameters, including the apparent persistence length and the radius of the chain, are tabulated in Table 2. The persistence length of DP10-PPV at a concentration of 0.1 wt % is 6.4 nm, which is about the same as that obtained from SLS for the dilute chloroform solution. Over the concentration range shown in Figure 2, the persistence length is found to increase with increasing concentration. The concentration dependence of the chain rigidity may be attributed to the excluded volume interaction between the rigid segments constituting the polymer chains, which is analogous to the excluded volume interaction between rodlike molecules that eventually leads to the formation of a nematic phase in the solution state at high concentration. At higher concentration, the relatively close distance between individual chains limits their rotational and translational degree of freedom in solution and hence forces the chains to stretch more.[17,18] This behavior is different from the conformational feature of flexible polymer coils, where the chains are expanded in good solvent but eventually reach their unperturbed dimensions at high concentration.

We have also attempted to reveal the wormlike chain conformation of DP10-PPV dissolved in chloroform by the real-space observation of the polymer chains using atomic force microscopy (AFM). The AFM samples were prepared by drop-casting the 0.008 mg/mL DP10-PPV/chloroform solution on a highly ordered pyrolytic graphite (HOPG). To arrest the wormlike structure of the polymer chains in the dilute solution, the solvent was evaporated very rapidly by blowing a nitrogen gas stream over the solution droplet during the casting. This procedure allows the chloroform solvent to be removed within 2 s. The polymer chains on the HOPG substrate were subsequently observed by a Seiko

(38) Sheiko, S. S.; Moller, M. *Chem. Rev.* **2001**, *101*, 4099.
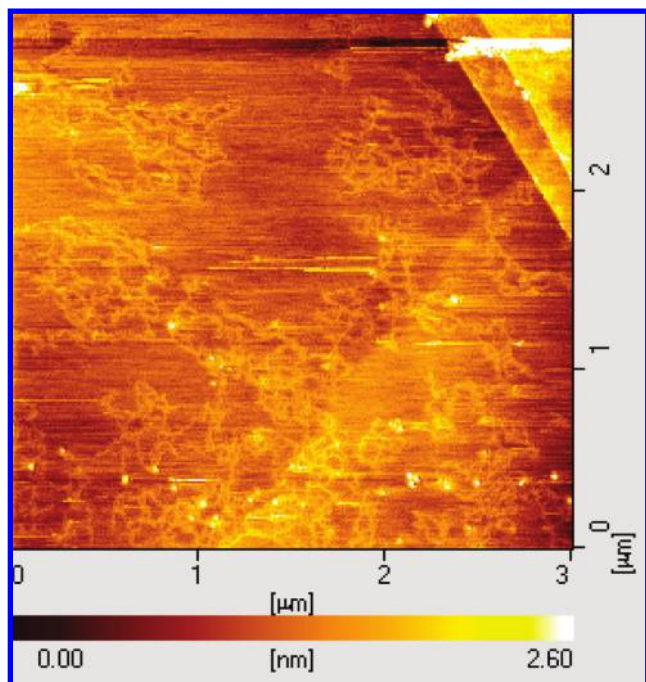
Figure 3. AFM topographic image of DP10-PPV cast from 0.008 mg/mL chloroform solution on HPOG. The dispersed wormlike coil structure several micrometers in size and some segmental associates formed by the polymer chains are observed over a large area.
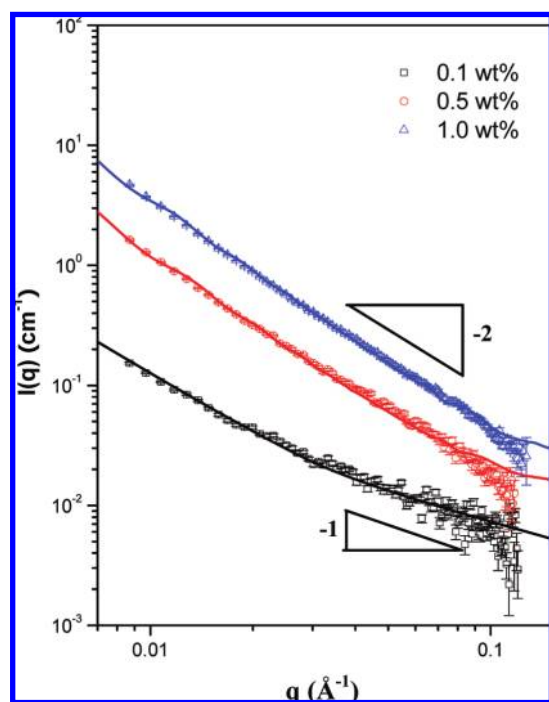

Figure 4. Room-temperature SANS profiles of DP10-PPV in toluene solutions at different polymer concentrations. The intensities exhibit a power law of $I(q) \sim q^{-2}$ at the higher concentrations of 0.5 and 1.0 wt % over nearly the entire *q* range studied. The SANS intensities at these two concentrations are considered to be dominated by the internal structure of the aggregates formed in toluene, where the micrometer-sized aggregates contain sheetlike nanodomains. The solid curves superposing on the corresponding scattering profiles represent the fits using the form factor of randomly oriented disks. The SANS profile of 0.1 wt % solution is considered to be dominated by the form factor of the wormlike DP10-PPV chains and the solid curve superposing on the experimental data corresponds to the fit using the wormlike chain model with excluded volume interaction.
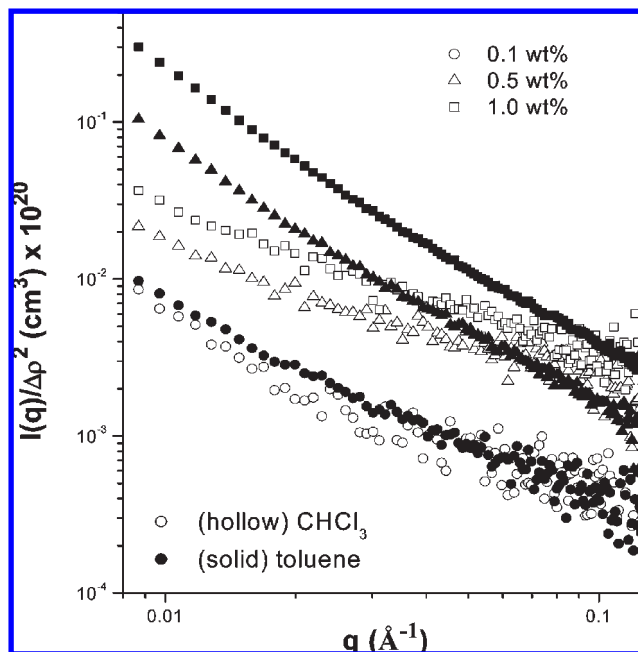

Figure 5. Contrast-normalized SANS profiles of DP10-PPV dissolved in toluene and chloroform. The normalized intensities of the toluene solutions are obviously higher than those of the corresponding chloroform solutions for concentrations of 0.5 and 1.0 wt %, whereas the contrast-normalized SANS profile superposes quite well with that of the chloroform solution for the 0.1 wt % toluene solution.

For the 0.1 wt % solution, the contrast-normalized SANS profile superposes quite well with that of the chloroform solution, showing that the aggregation is minor, and the SANS profile is still dominated by the form factor of the worm-like chain. The corresponding fitting using the worm-like chain model yields the persistence length of 5.5 nm. This value is smaller than that found for DP10-PPV in chloroform at the same concentration, which is consistent with the SLS results, suggesting that the polymer chains adopt a more expanded conformation in chloroform.

When the concentration is increased to 0.5 and 1.0 wt %, the scattering intensities display q^{-2} power law, which suggests that the micrometer-sized aggregates of DP10-PPV contain sheetlike nanodomains. The solid curves superposing on the corresponding scattering profiles in Figure 4 represent the fits using the form factor of randomly oriented disks (see Supporting Information for the equation of the form factor of disk). This fitting yields the thickness of the sheetlike domains of ca. 2.0 nm, irrespective of the concentration. It should be noted that, although the R_g of the sheetlike domains can be obtained from the fittings, the values are not considered to be highly meaningful, because the Guinier region is not accessed under the *q* range studied. The value of the thickness, which is determined by the scattering profile in the high-*q* region, is nevertheless reliable.

Considering the fact that the diameter of the DP10-PPV chain obtained from the fitting using the wormlike chain model is ca. 9 Å, the sheetlike nanodomains in the aggregates may consist of a bilayer of DP10-PPV chains lying flatly on the sheet surface, as schematically shown in Figure 6. Similar sheetlike domains formed by the segmental aggregation have also been observed for other conjugated polymers such as poly(2-methoxy-5-(2'-ethyl-hexyloxy)-1,4-phenylene vinylene)
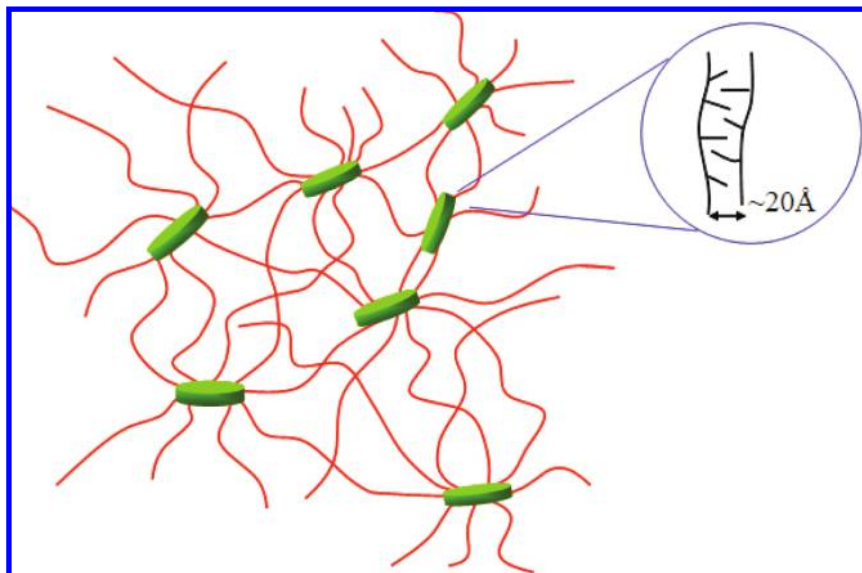
Figure 6. Schematic illustration of the structure of the aggregates of DP10-PPV in toluene. The micrometer-sized aggregates are proposed to contain sheetlike nanodomains ca. 2.0 nm thick consisting of a bilayer of DP10-PPV chains lying flatly on the sheet surface.

(MEH-PPV)[34] and polyfluorenes[39,40] dissolved in relatively poor solvents. Our previous study of DP6-PPV revealed that the aggregates in toluene tended to collapse into disklike objects as a result of severe segmental association.[22] These results imply a general tendency of hairy-rod conjugated polymers to aggregate to form a sheetlike domain, which is micellar in nature in relatively poor solvents. Indeed, a recent theoretical study of the phase behavior of hairy-rod polymers by Knaapila et al. has predicted the existence of a membrane phase in which the polymer chains packed to form bilayered sheets over a narrow temperature range, while the nematic−isotropic coexistence is found to dominate the phase diagram in the phase-separated region.[40] Although the system tends to demix upon lowering the temperature, the phase separation occurs very slowly because of the network of the membranes already existing in the solution. Consequently, the formation of the sheetlike membrane may supersede the lyotropic−isotropic demixing, and the metastable membrane structure is eventually kinetically arrested.

3. Dynamic Behavior Probed by DLS. DLS has been employed here to probe the dynamic behavior of DP10-PPV in solutions with chloroform and toluene, from which the dispersion state of the polymer is further elucidated. In the dilute regime where the interaction between the polymer chains is insignificant, DLS probes the translational motion of the individual chains; as such, the correlation length corresponds to the average hydrodynamic radius of the polymer chains. In the semidilute regime, the relaxation rate of the polymer is slowed down because the mobility of the chain segments is constrained by each other.[41,42] An even slower relaxation mode associated with the motion of the

clusters can be identified when the polymer chains undergo aggregation in the solution.

Figure 7 displays the normalized intensity correlation function (collected at $\theta = 90°$) and the R_h distribution of DP10-PPV in chloroform and toluene solutions at different concentrations. With the increase of concentration, the correlation function is found to shift to longer time along the relaxation time axis. The decay in the autocorrelation function at a delay time of $< 1 \mu s$ is attributed to the motion of the flexible side chains attached to the conjugated backbone of DP10-PPV. The R_h spectra reveal that, in the solutions with concentrations of ≤ 0.05 wt %, DP10-PPV in both chloroform and toluene solutions exhibit only a bimodal relaxation with the fast and the intermediate modes. The fast mode with the average R_h of about 0.1 nm represents the motion of the flexible side chains, while the intermediate mode is attributed to the translational diffusion of individual DP10-PPV chains. In this case, the hydrodynamic radius does not show any remarkable change with increasing concentration, reflecting the free motion of the flexible side chains and the free translational diffusion of the individual chains due to the absence of interchain aggregation. With the increase of concentration, the interaction between the chain segments becomes stronger and hence limits the mobility of the chain segments, thereby leading to increased R_h of individual DP10-PPV chains with concentration. This is reminiscent of the SANS results showing the increase of l_p with increasing concentration due to increased excluded volume interaction.

As the concentration exceeds 0.05 wt%, an additional slow relaxation mode with a corresponding R_h of ca. 200 nm to 10 μm is observed. This slow mode is considered to be contributed by the aggregates of DP10-PPV. However, the fact that the population of this mode is small compared with the that of the intermediate mode for the chloroform solutions and the 0.1 wt % toluene solution indicates that the interchain aggregation is not significant, such that the corresponding SANS profiles are still dominated by the form factor of the molecularly dissolved wormlike chains.

On the other hand, the slow mode dominates the relaxation spectra for 0.5 and 1.0 wt % toluene solutions,

(39) Knaapila, M.; Dias, F. B.; Garamus, V. M.; Almásy, L.; Torkkeli, M.; Leppänen, K.; Galbrecht, F.; Preis, E.; Burrows, H. D.; Scherf, U.; Monkman, A. P. *Macromolecules* **2007**, *40*, 9398.
(40) Knaapila, M.; Stepanyan, R.; Torkkeli, M.; Garamus, V. M.; Galbrecht, F.; Nehls, B. S.; Preis, E.; Scherf, U.; Monkman, A. P. *Phys. Rev. E* **2008**, *77*, 051803.
(41) Amis, E. J.; Janmey, P. A.; Ferry, J. D.; Yu, H. *Macromolecules* **1983**, *16*, 441.
(42) Teraoka, I. *Polymer Solutions: An Introduction to Physical Properties*; John Wiley & Sons: New York, **2002**.
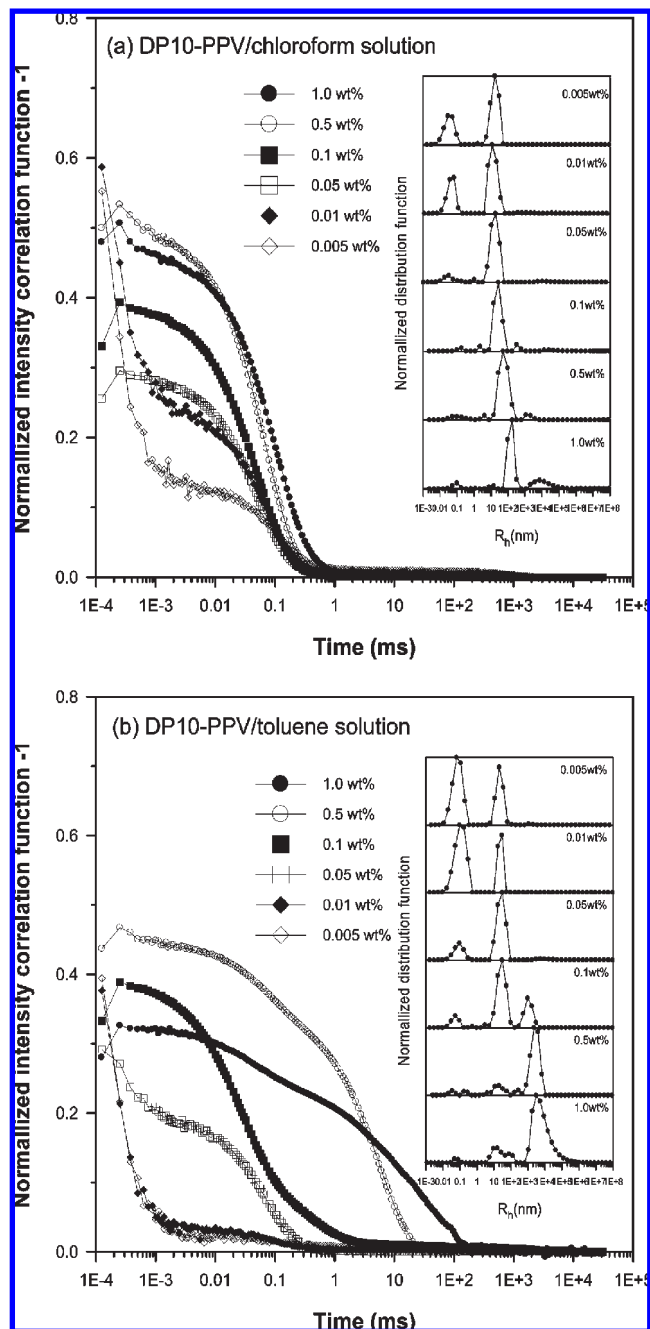
Figure 7. Normalized intensity correlation functions, $g^2(t)-1$ of DP10-PPV in solutions at different concentrations collected at $\theta = 90\,^\circ$ and at 25 °C: (a) DP10-PPV/chloroform solutions, and (b) DP10-PPV/toluene solutions. Insets: Corresponding hydrodynamic radius (R_h) distributions.

which is consistent with the foregoing postulate that the corresponding SANS profiles are dominated by the aggregates. In this case, the R_h value of the slow mode is considered as a measure of the size of the clusters or microgel networks originating from the segmental association that yields the sheetlike nanodomains acting as the physical cross-links for the microgel networks. Consequently, in contrast to chloroform solutions where the segmental association is not so severe, the amplitudes of the fast and the intermediate relaxation modes reduce remarkably as a result of the formation of the aggregate structures, and the slow mode becomes the dominant relaxation mode for the 0.5 and 1.0 wt % toluene solutions.

Recently, we reported the aggregation behavior of DP6-PPV in the solution state.[22] This polymer with hexyl side chains shows a strong interchain aggregation even in chloroform, and the network aggregates thus generated dominate the SANS intensity. However, the present study has demonstrated that a major fraction of DP10-PPV chains remain well dispersed in chloroform, indicating that increasing the length of the flexible side chains attached to the PPV backbone tends to suppress the interchain aggregation. The effect of side-chain length that results in different dissolution behavior is further demonstrated by comparing SANS intensities normalized by the corresponding neutron SLD contrasts of the two polymers, $I(q)/\Delta\rho^2$, as shown in Figure 8 for the 1.0 wt % solution. It can be seen that DP6-PPV clearly shows a much stronger intensity in the low-q region, which is consistent with a much more severe interchain aggregation in solution. For DP6-PPV, we have proposed that the aggregation observed in the chloroform solution stems primarily from incomplete dissolution of a fraction of the hairy-rod segments of the polymer. This fraction in fact forms highly a stable $\pi-\pi$ complex in the solid DP6-PPV powder used for solution preparation.[22] This kind of $\pi-\pi$ complex is formed by in-plane stacking of the phenylene or the phenyl moieties in DP6-PPV, and a characteristic distance of ca. 3.0Å between the aromatic groups forming the complex leads to a peak at $2\theta \approx 29°$ in its wide-angle X-ray scattering (WAXS) profile.[43] This species could neither be solvated by chloroform nor be disrupted by heating; as a result, the chains tied firmly by the $\pi-\pi$ complex form the network aggregates in the solution.

Because of its longer flexible side chains, DP10-PPV remains well dispersed in chloroform. Thus we may speculate that the highly stable $\pi-\pi$ complex found in DP6-PPV may be absent in the DP10-PPV powder. This assumption is corroborated by Figure 9, which compares the WAXS profiles of DP10-PPV powder with that of DP6-PPV powder. It can be seen that DP6-PPV displays a higher degree of crystallinity and shows a strong scattering peak at $2\theta = 29°$ (corresponding to a Bragg spacing of 3.0 Å) associated with the $\pi-\pi$ complex. This peak is however missing in the WAXS profile of DP10-PPV powder, indicating the lack of $\pi-\pi$ complex formation in this polymer. In this case, the stronger steric hindrance imposed by the longer decyl side chains in DP10-PPV may impede the complex formation in the powder. Hence, a uniform dispersion of polymer chains in chloroform becomes accessible for DP10-PPV.

4. Disruption of the Aggregates of DP10-PPV in Toluene Solution by Heating. According to our previous study of DP6-PPV, the micelle-like segmental association formed in toluene is relatively unstable, as it can be disrupted by moderate heating.[22] Figure 10 shows a series of SANS profiles of 1.0 wt % DP10-PPV/toluene solution collected in situ at various temperatures in a heating process. The scattering intensity in the low-q region drops suddenly when the temperature is increased to 55 °C, showing the occurrence of deaggregation upon heating, similar to the DP6-PPV system. Also, the q^{-1} power law emerges in the high-q region as a result of the increased population of the molecularly dissolved chains. Heating to 70 °C completely wipes out the segmental aggregation, as the scattering profile at this

(43) Huang, Y. F.; Yang, S. H.; Hsu, C. S.; Chen, S. A.; Su, A. C. *ICMAT International Conference on Materials for Advanced Technologies*, Singapore **2001**.
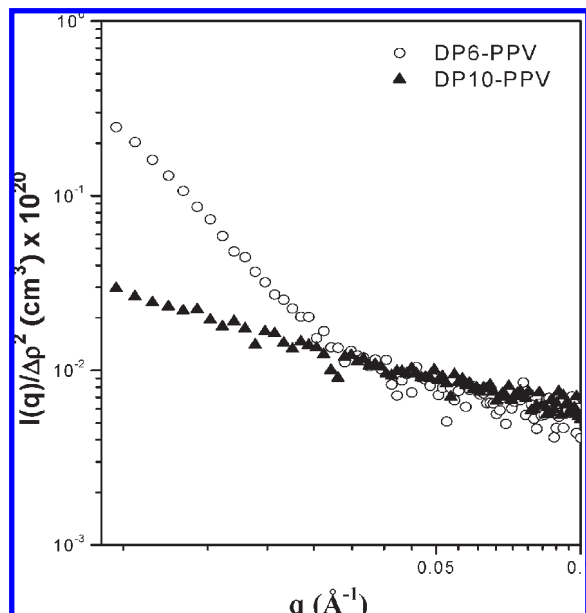
Figure 8. Comparison between the contrast-normalized SANS intensities of 1.0 wt % DP6-PPV and DP10-PPV solutions in chloroform. The much stronger low-q intensity of the DP6-PPV solution is due to a significant degree of interchain aggregation.
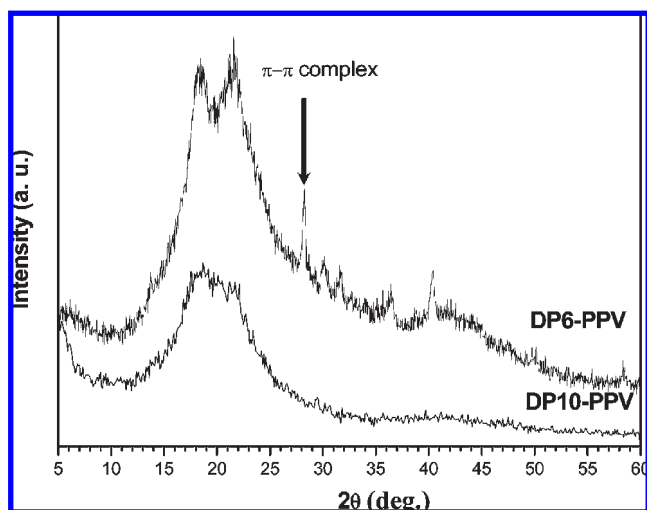

Figure 9. WAXS profiles of DP6-PPV and DP10-PPV powders. DP6-PPV powder is seen to exhibit a strong peak at $2\theta = 29°$ (corresponding to a Bragg spacing of 3.0 Å) associated with the $\pi-\pi$ complexes in the powder. This peak is essentially missing in the WAXS profile of DP10-PPV.

Figure 10. SANS profiles of 1.0 wt % DP10-PPV/toluene solution collected in a heating cycle. Inset: The corresponding SANS profiles normalized by the SLD contrasts of 1.0 wt % solutions of DP10-PPV with chloroform (25 °C) and toluene solutions (85 °C), showing that the contrast-normalized scattering profiles of these two solutions match quite well.

Figure 11. SANS profiles of 1.0 wt % DP10-PPV/toluene solution obtained by a heating−cooling cycle between 25 and 85 °C.

temperature nearly matches that collected at an even higher temperature, 85 °C. It is interesting to note that the contrast-normalized scattering profiles at these temperatures closely match that of the 1.0 wt % chloroform solution at room temperature (inset of Figure 10), where the scattering profile is dominated by the form factor of DP10-PPV chains. After the data acquisition at 85 °C, the toluene solution was cooled right back to 25 °C to examine the reaggregation behavior of DP10-PPV. The SANS profile of the cooled solution collected within 1 h after reaching 25 °C is shown in Figure 11. Although the low-q intensity increases slightly upon cooling, the scattering profile does not recover to that of the as-prepared solution (which has been stored at 25 °C for more than 24 h prior to SANS experiment), indicating that the reaggregation is spontaneous but slow.
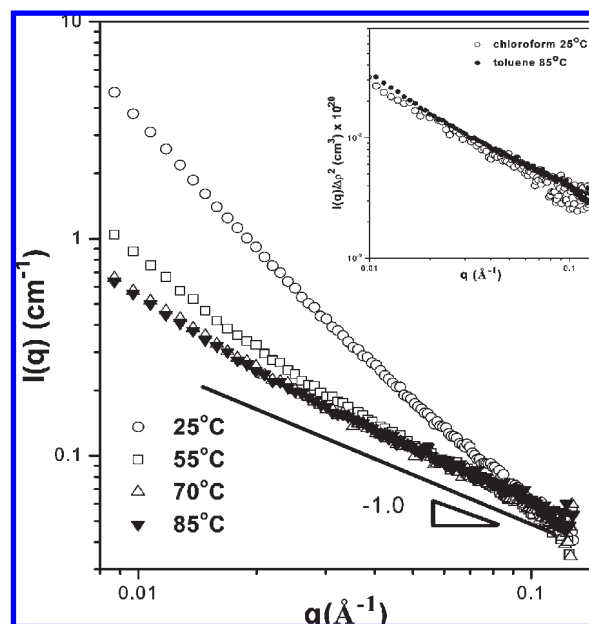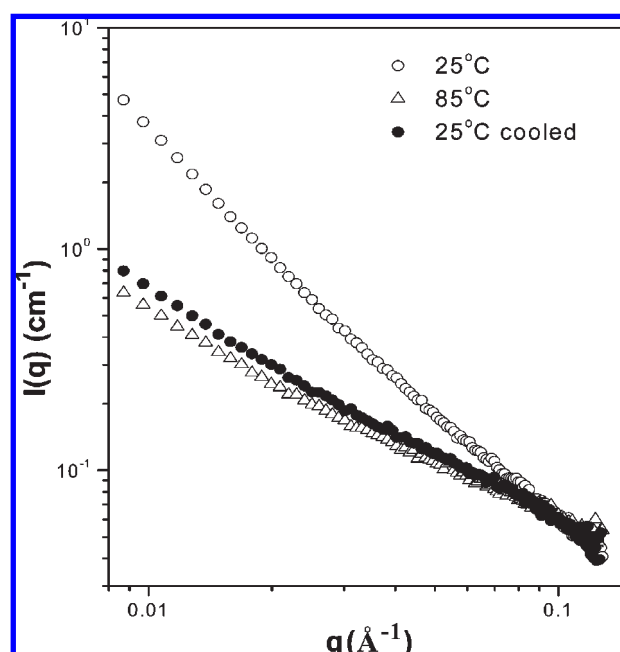
Figure 12 shows the temperature dependences of the light scattering intensity measured at 90° (which is mainly contributed by the molecularly dissolved chains due to large scattering angle) and the R_h distribution (inset of Figure 12) of 0.5 wt % DP10-PPV/toluene solution obtained by DLS in an in situ heating at the rate of 0.5 °C/min. As the temperature is increased, the scattering intensity increases remarkably, while the amplitude of the slow mode of the R_h distribution associated with the aggregates decreases drastically and shifts to lower R_h values. These observations indicate that the extent of interchain aggregation decreases at
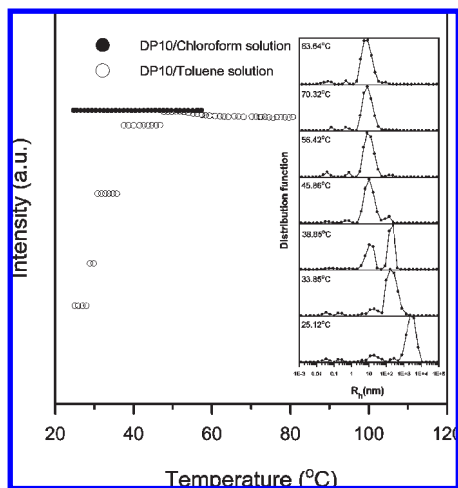
Figure 12. DLS intensity of 0.5 wt % DP10-PPV solutions obtained at various temperatures in a heating process with the heating rate of 0.5 °C/min. Inset: Corresponding R_h profiles of 0.5 wt % DP10-PPV/toluene solution display three peaks, each stemming from a characteristic relaxation mode in the system.

higher temperatures, and the slow mode finally vanishes above 45 °C. Meanwhile, the amplitude of the intermediate mode associated with the dynamics of individual DP10-PPV worm-like chains increases with increasing temperature, as a result of an increase in the concentration of molecularly dispersed DP10-PPV chains arising from the disintegration of the intermolecular aggregates on heating. These results imply that the micelle-like segmental association of DP10-PPV in toluene solutions is rather weak, as it can be disrupted by moderate heating. This is in identical with that found for DP6-PPV/toluene solutions.

Conclusions

We have investigated the effects of solvent quality, concentration, and temperature on the conformational structure and the interchain aggregation behavior of DP10-PPV in solutions with chloroform and toluene by SANS, SLS, and DLS. The polymer−solvent interaction between DP10-PPV and chloroform was stronger than that between DP10-PPV and toluene; consequently, in dilute solutions, the DP10-PPV chains assumed a more extended wormlike conformation

in chloroform. The persistence length of DP10-PPV in chloroform was found to increase with increasing concentration due to the excluded volume interaction. The interchain aggregation started to set in as the concentration exceeded 0.1 wt % in both solutions. The extent of aggregation was, however, minor in chloroform but became significant in toluene solutions with concentrations of ≥0.5 wt%. The aggregation gave rise a slow relaxation mode with a corresponding hydrodynamic radius of 200 nm to 10 μm as measured by DLS. This relaxation mode was attributed to the formation of micrometer-sized clusters or microgel networks in which a fraction of the hairy-rod segments associated to form sheetlike nanodomains that acted as the physical cross-links for the networks. Nearly all aggregates of DP10-PPV in toluene solutions could be disintegrated by moderate heating. This was in clear distinction from DP6-PPV, where a fraction of the segments of DP6-PPV formed highly stable $\pi-\pi$ complexes in the solid powder, and such a strong segmental association (that could neither be solvated by chloroform nor be disrupted by heating) persisted in the solution state. The strong $\pi-\pi$ complex was absent in DP10-PPV because the longer decyl side chain imposed a large steric effect, preventing the effective in-plane stacking of the phenylene or the phenyl moieties in DP10-PPV.

Supporting Information Available: SANS intensity profiles normalized by the overall polymer concentration of DP10-PPV/chloroform solutions; theoretical analysis of the thermodynamics and phase behavior of DP6-PPV solutions; the expression of the scattering intensity of the wormlike chain model with excluded volume interaction; the equation of the form factor of randomly oriented disk. This material is available free of charge via the Internet at http://pubs.acs.org.